Volume 1 | Number 1 | Jan 2013 | Pages 1–100

Organic & Biomolecular Chemistry

www.rsc.org/obc

ROYAL SOCIETY OF CHEMISTRY

www.rsc.org/obc

ARTICLE TYPE

Evaluation of 4-substituted styrenes as functional monomers for the synthesis of theophylline-specific molecularly imprinted polymers

Hazit Zayas,[a] Clovia I Holdsworth,[a] Michael C Bowyer [b] and Adam McCluskey[a*]

Abstract: Six novel functional monomers: 4-(4-vinylphenyl)pyridine (**M1**), 4'-vinylbiphenyl-4-ol (**M2**), N,N-dimethyl-4'-vinylbiphenyl-3-amine (**M3**), (4'-vinylbiphenyl-4-yl)methanol (**M4**), 4'-vinylbiphenyl-4-carboxylic acid (**M5**) and 4-hydroxy-5-methyl-4'-vinylbiphenyl-3-carboxylic acid (**M6**), were examined
10 for their ability to imprint theophylline (**1**). Using a molecular modelling-NMR titration approach **M2** and **M6** were predicted to give rise to the most specific molecularly imprinted polymers (MIPs). Rebinding analysis suggests that no imprinting effect resulted from the polymerisation of monomers **M1**, **M5** and **M6**, but modest to good levels of imprinting were evident from monomers **M2**, **M3** and **M4** with IF values ranging from 1.1 (MIP$_{M3}$, 20 mg) to 45 (MIP$_{M2}$, 10 mg). The selective recognition of **1** varied as a
15 function of polymer mass used. At low polymer loadings MIP$_{M2}$ gave the very high IF of 45, reducing to IF = 4.1-2.3 at 20-40 mg polymer loading. With monomer **M2** microwave synthesis MIP (MW-MIP$_{M2}$) synthesis was examined. The MW-MIP$_{M2}$ displayed lower specific rebinding than its conventionally produced counterpart (MIP$_{M2}$) with IF values ranging from 1.6-2.3 (c.f., MIP$_{M2}$ IF 2.3-45), but significantly higher levels of rebinding with 25-52% of **1** rebound from a 0.080 mM CH$_3$CN solution of **1**
20 (c.f., MIP$_{M2}$ 5-25%). MW-MIP$_{M2}$ displayed a lower BET surface area than MIP$_{M2}$ (185 m^2/g vs. 240 m^2/g), lower surface (Zeta) potential (-13.1 ± 8.22 mV vs. -31.4 ±4.84 mV). Freundlich isotherm analysis revealed that MW-MIP$_{M2}$ possessed higher affinity binding sites for **1** than MIP$_{M2}$ with K_d values of 1.38 and 2.31 respectively. In addition MW-MIP$_{M2}$ also exhibits a higher number of binding sites (N_T) compared to MW-NIP$_{M2}$ (0.72 and 0.41 mg/g, respectively). In specificity studies using caffeine (**2**)
25 MIPM2 displayed a two-fold preference for rebinding of **1** and MW-MIP$_{M2}$ a five-fold preference for **1** over **2**. The quantity of **2** bound in both cases was consistent with non-specific binding events. In competitive rebinding experiments increased discrimination in favour of **1** over **2** was observed.

Introduction

Molecularly imprinted polymers (MIPs) are a class of specialty
30 macromolecules that retain a memory of the template used in their synthesis.[1] This template memory results in a potential for highly specific rebinding of the original template and closely related analogues, affording easy removal from solution and if required, detection and quantification.[2-4] These properties,
35 combined with their relative ease of synthesis, have seen a proliferation of application of MIPs in chemo- and bio-sensors.[4-14] After rebinding, template extraction allows easy identification and quantification. MIPs can be utilised as highly specific solid phase extraction systems allowing analyte concentration and
40 quantification via traditional chromatographic technologies. However, there is an emerging technology that sees MIPs coupled to a wide variety of electronic reporter systems. MIP and their application in sensors, in analyte detection and in drug delivery have been extensively reviewed.[4,15-18]
45 Traditionally, MIPs are synthesized by the polymerisation of a solution that comprises a template (T; the analyte), a functional monomer (FM; the specific recognition element), a crosslinking

agent (CL; to impart structural integrity which also plays a role in enhancing specificity) and a porogen (a solvent).[1,3,19-24] In the
50 design considerations that lead to MIP synthesis, the FM is arguably the most important element that imparts specific recognition as it is the interactions between the FM and T that generate the characteristic features within the resultant polymer cavity required to facilitate template rebinding. Over the past 2-3
55 decades, there have been multiple reports of novel (and traditional) functional monomers that have been successfully used the preparation of highly efficacious MIPs.[1,3,4,15-34]

MIPs have often been compared to biological systems such as enzymes and antibodies, but as yet, we are unaware of any study
60 that has utilised the basic biological recognition element, the amino acid, as a strategy for designing novel FMs for MIP synthesis. While there are twenty naturally occurring amino acids these are routinely grouped together into polar, non-polar, acidic and basic amino acids, simplifying the actual number of
65 recognition elements used in nature. Indeed Walter *et al.* have reported the synthesis of a fully functioning AroQ chorismate mutase homologue with a vastly simplified 9-letter amino acid alphabet.[35] We thus set about designing a minimalist library of

polymerisable amino acid surrogates. In our initial design criteria, we sought to have ease of synthesis and complementarity of functional groups and pK$_a$ as the key ingredients. From this, we designed six substituted styrene functional monomers (Figure 1). These monomers were readily accessed through a microwave assisted Suzuki couplings.[36]
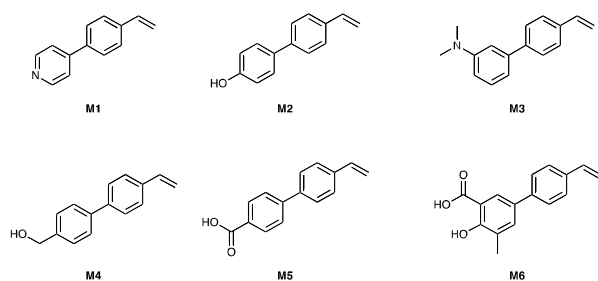

Figure 1. Chemical structures of a six member 4-substituted styrene functional monomer library; 4-(4-vinylphenyl)pyridine (**M1**), 4'-vinylbiphenyl-4-ol (**M2**), N,N-dimethyl-4'-vinylbiphenyl-3-amine (**M3**), (4'-vinylbiphenyl-4-yl)methanol (**M4**), 4'-vinylbiphenyl-4-carboxylic acid (**M5**) and 4-hydroxy-5-methyl-4'-vinylbiphenyl-3-carboxylic acid (**M6**).

Herein, we explore the evaluation of **M1-M6** as novel functional monomers for the synthesis of theophylline specific MIPs. Theophylline is a widely used drug for treatment of asthma; however, its use has continually declined over the years due to its adverse health effects and toxicity.[37] This has limited the use of theophylline (**1**) (Figure 2) and requires regular monitoring of theophylline levels in blood or urine, usually determined and quantified via conventional chromatography.[38,39]

As an alternative, several **1**-imprinted polymers have been successfully used to determine the concentration of **1** in human serum samples.[38-41] These **1**-imprinted polymers were used as solid phase sorbents in solid phase extraction or micro columns,[38,39] and as a sorbent in ligand binding assays.[40] So far, **1**-selective MIPs have been prepared using methacrylic acid (MAA) as functional monomer, taking advantage of its strong interactions with **1** (via hydrogen bonding) favouring the formation of stable T:FM clusters and, subsequently, the formation of stable target-specific cavities. The biphenyl monomers utilised in this study also possess functional groups capable of interaction with **1**, and their potential as functional monomers, i.e. formation of stable T:FM clusters, are evaluated herein for the first time.
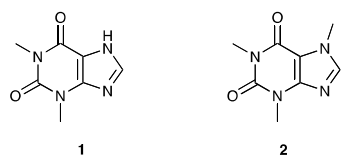

Figure 2. Chemical structure of theophylline (**1**) and the related caffeine (**2**).

Results and Discussion

Application of a combination of molecular modelling and NMR titration analysis to the interactions between the template and functional monomers, a MM-NMR approach,[4,13,14] highlighted potentially favourable interactions between **1** and all six novel monomers (**M1-M6**, ESI†). As is common with MM-NMR analysis, each template was examined in turn as a single component interacting with the template. The modelling and NMR studies supported, for monomer **M1** a T:FM ratio 3:1; for monomer **M2** a 1:2 to 1:5; for monomer **M3** a 2:3; for monomer **M4** a 1:1; for monomer **M5** a 2:3; and for **M6** a 1:2 for the pre-polymerisation clusters. In all instances strong hydrogen bonds

(< 2.5 Å) and π-π interactions were evident (ESI†).

Modelling of **1-M1** clusters supported a single point of interaction for hydrogen bonding between the theophylline –NH proton and the **M1** pyridyl nitrogen. Maximum favourable interactions were observed at 1:3 T:FM cluster ratio (ESI†). The Job plots of theophylline suggested the existence of a mixture of T:FM complexes showing a maximum at ~1:2 (ESI†). The existence of a maximum when **1** > **M1** was attributed to inter-template interactions. Modelling of **1-M2** indicates a strong interaction between both species with the Job plots suggesting a mixture of T:FM complexes with ratios of ~1:2 and 1:5 were favoured (ESI†). The **1-M3** cluster interaction gave rise to the lowest energy of interaction of the monomers examined (Table 1). Like **M1**, **M3** was only capable of acting as a hydrogen bond acceptor. With **M3**, our modelling analysis supported a theophylline-NH to -N(CH$_3$)$_2$ **M3** H-bond. The Job plot supported a 2:3 T:FM ratio (ESI†).

The $\Delta E°_{(cluster)}$ values for the **1-M4** clusters showed comparable levels of interaction to that of **1-M2**; however, unlike **M2**, modelling suggested that, while T:M ratios higher than 1:1 allowed more **1-M4** hydrogen bonding interactions to form, unfavourable FM-FM interactions dominated. The Job plots for **1-M4** favoured a 1:1 – 1:2 T:FM cluster ratio.

Of all the vinyl biphenyl monomers evaluated, **M6** gave the highest $\Delta E°_{(cluster)}$ values (ESI†). As with **M4**, **M6** was also a hydrogen bond donor and acceptor capable of forming multiple hydrogen bonds with theophylline (ESI†). The **1-M6** Job plots were consistent with a strong interaction at a T:FM ratio of 1:4. The level of **1-M6** interaction started to plateau at a T:FM ratio of 1:4, with further addition of **M6** failed to enhance the **1-M6** interactions with **M6-M6** interactions increasingly evident. Overall the **1-M6** Job plot supported a maximal T:FM interaction ratio of 1:1.5.

Overall the T:FM interaction studies suggest that **M1-M6** were capable of interacting favourably with theophylline through hydrogen bonding. Both molecular modelling and ^{1}H NMR spectroscopy approaches supported potentially favourable T:FM interactions with minimal inter-monomer association achieved at T:FM ratios ≤ 1:4. Among the six monomers studied, **M2** and **M6** gave the highest T:FM complex induced NMR shifts, as highlighted by the Job plots with **1** at mole fractions of < 0.5, and suggested that the interaction of **M2** and **M6** with **1** was stronger than with the other functional monomers.

Synthesis and Characterisation of 1-MIPs

Previous approaches for **1**-based MIPs used a combination of MAA and ethylene glycol dimethacrylate (EGDMA) as the crosslinker.[38,40-45] Herein EGDMA was retained as the crosslinker and **M1-M6** evaluated as MAA replacements. Imprinted and non-imprinted control polymers incorporating FMs **M1-M6** were prepared by traditional thermal polymerisation,[40,42,45] for preliminary assessment of rebinding properties, with the best performing formulation(s) then comparatively assessed against their microwave synthesised counterparts. Each MIP and the corresponding non-imprinted polymer (NIP) was ground and sieved to 38 μm prior to use. The MIPs synthesised thermally exhibited good (2.0x; **1-M4**) to excellent (5.0x; **1-M5**) levels of swelling in acetonitrile, the rebinding porogen (ESI†). SEM evaluation of each of these systems also suggested a high level of surface porosity (Figure 3).

To determine the efficacy of each MIP generated from **M1-M6**, a series of rebinding experiments were conducted using a stock solution of **1** in acetonitrile (0.0800 mM, V = 1.00 mL). MIP efficacy was measured as an imprinting factor (*IF*), where

IF = [Template rebound by MIP] / [Template rebound by NIP]. Varying amounts of MIPs and NIPs for each set of polymers were used to bind a constant amount of template over a constant binding period (18 h) using 1.00 mL of 0.080 mM theophylline in acetonitrile. The concentration of free (unbound) theophylline was determined by HPLC, and the calculated IF values are presented in Table 1.

Table 1. Comparison of the specific rebinding (IF values) for the synthesised MIPs (MIP$_{M1}$-MIP$_{M6}$) across a range of polymer masses at a fixed rebinding stock solution of 0.0800 mM **1** in CH$_3$CN. Rebinding time = 18 h.

MIP	MIP Mass (mg)			
	10	20	30	40
	IF			
MIP$_{M1}$	2.7	1.0	1.2	1.0
MIP$_{M2}$	45	4.1	3.7	2.3
MIP$_{M3}$	-[a]	2.2	1.1	1.4
MIP$_{M4}$	-	-	0.7	3.8
MIP$_{M5}$	0.8	1.0	1.0	1.0
MIP$_{M6}$	0.9	1.0	1.0	1.0

[a] - = not determined

The data presented in Table 1 suggests that no imprinting effect resulted from the polymerisation of monomers **M1**, **M5** and **M6**, but modest to good levels of imprinting were evident from monomers **M2**, **M3** and **M4** with IF values ranging from 1.1 (MIP$_{M3}$, 20 mg) to 45 (MIP$_{M2}$, 10 mg). The selective recognition of **1** varied as a function of polymer mass used. At low polymer loadings MIP$_{M2}$ gave the very high *IF* of 45 (average of three replicates), reducing to the more normal 4.1-2.3 at 20-40 mg polymer loading. This was most likely a function of increasing non-specific binding, in turn a consequence of increased surface area and binding site availability. MIP$_{M3}$ and MIP$_{M4}$ returned best IF values of 2.2 and 3.8 at polymer loadings of 20 mg and 40 mg respectively.

Our findings with **M1** and **M5** were consistent with the MM-NMR studies of these FMs with **1**. This was also the case with **M3** in MIP$_{M3}$, as it contained a bulky dimethylamino moiety that our modelling analysis showed to be capable of only one-site interaction (H-bonding with proton 1) with **1**. However, **M6** in MIP$_{M6}$ was capable of not only of interacting with **1** at multiple sites but also showed intramolecular hydrogen bonding due to its *ortho* disposed carbonyl and hydroxy substituents, most likely favouring intra- rather than inter- molecular H-bonding. Both modelling and NMR results showed favourable interactions between **M4** and **1**, but this monomer failed to produce an effective MIP, presumably as the monomer-monomer interactions dominated in the pre-polymerisation cluster. Molecular modelling showed the dimerisation of **M6** and **M4** to be energetically more favourable than for **M2**, with ΔH^{o}_{f} values of -45 kcal.mol^{-1} for **M6** dimer, -20 kcal.mol^{-1} for **M4** dimer and -43 kcal.mol^{-1} for M2 dimer (ESI†). The presence of **M1** and **M6** enhanced the non-selective uptake of **1** and resulted in no binding discrimination between MIP and NIP. Only MIP$_{M2}$ exhibited an imprinting effect for **1**. It would appear that the phenolic moiety of **M2** enhanced its capability to form a stable T:M cluster for successful imprinting of **1**.

As we,[46] and others,[47] had previously demonstrated that the polymerisation temperature and mode of heating impacts on the quality and specificity of the resultant MIPs, we examined the effect of microwave heating on MIP production and efficacy with **M2**, the FM that displayed the most favourable thermal MIP properties. We have previously demonstrated that the imprinting of caffeine is enhanced under these conditions through the faster rate of polymerisation and 'snap freezing' of the imprints. In line with this area of investigation, microwave polymerisation was also applied to the study of **1**-imprinted polymers. These studies were limited to the **M2** functional monomer. A microwave synthesised MIP using **M2** was prepared (MW-MIP$_{M2}$), with the corresponding MW-NIP$_{M2}$ synthesised under the same conditions.

Examination of the specific rebinding characterisations of MW-MIP$_{M2}$ (and MW-NIP$_{M2}$) was conducted under identical conditions as used for the traditionally produced MIP$_{M2}$ and NIP$_{M2}$. The outcomes of these studies are presented in Table 2.

Table 2. Comparison of the specific rebinding (IF values) for the microwave synthesised MIP (MW-MIP$_{M2}$) and thermally synthesised MIP (MIP$_{M2}$) and the rebinding capacity of MW-MIP$_{M2}$ and MIP$_{M2}$. IF was determined using a fixed rebinding solution of 0.080 mM **1** in CH$_3$CN. Rebinding time = 18 h.

MIP	MIP Mass (mg)				MIP Mass (mg)			
	10	20	30	40	10	20	30	40
	IF values				%-**1** rebound			
MW-MIP$_{M2}$	1.6	2.3	2.3	1.7	25	41	52	48
MIP$_{M2}$	45	4.1	3.7	2.3	5	13	18	25

The IF values and degree of **1**-recovery plateau at 30 mg polymer loading suggesting that future studies should be carried out at this polymer loading (Table 2). The MW-MIP$_{M2}$ displayed lower specific rebinding than MIP$_{M2}$ with IF values ranging from 1.6-2.3 (c.f., MIP$_{M2}$ IF 2.3-45), but significantly higher levels of rebinding with 25-52% of **1** rebound (c.f., MIP$_{M2}$ 5-25%). This was due to a significantly enhanced non-specific binding of MW-NIP$_{M2}$ (data not shown).

In an effort to determine the root cause of this enhanced binding capacity, we examined a wide range of physical characteristics associated with the gross polymer structure. From IR analysis we noted no significant difference between MW-MIP$_{M2}$'s and MW-NIP$_{M2}$'s and between thermal and microwave polymers (ESI†). All spectra show the presence of unreacted CL. In particular, the peak at ($\upsilon_{C=C}$ ~1605 cm^{-1}) and correlation of this peak with $\upsilon_{C=O}$ (~1760 cm^{-1}) suggests a slightly lower degree of crosslinking in thermal polymers than for the microwave polymers. This in turn impacts on MIP specificity.[48,49] The swelling capacity of both microwave and thermal polymers were determine (data not shown). Although both thermal and microwave polymers exhibited similar swelling, the microwave polymers are found to bind more **1** than the thermal polymers.

BET surface area analysis using CO$_2$ (as efforts with N$_2$ were unsuccessful) gave insight to the specific surface area and pore size distribution of micropores (Table 3).[50] While the difference in gas adsorption between MIP$_{M2}$ and NIP$_{M2}$ was minimal, there were significant differences between the adsorption isotherm of MW-MIP$_{M2}$ and that of MW-NIP$_{M2}$, neither of which resembles the adsorption isotherms of the thermal polymers (Figure 4). At a relatively low pressure, there was a rapid increase in the volume of gas adsorbed by the MW-MIP$_{M2}$ as indicated by the "knee" in the isotherm and this represents rapid monolayer adsorption at the micropore region of the MW-MIP$_{M2}$ polymer.[51] The MW-NIP$_{M2}$ displayed a higher volume of gas adsorbed at the same relative pressure which indicated that MW-MIP$_{M2}$ had a higher microporosity than MW-NIP$_{M2}$. The two sharp maxima at < 10 Å are consistent with MW-MIP$_{M2}$ containing pseudo-monodisperse pores located displaying of 1-2 Å in size. The pore sizes observed with the other three polymers was random, with no concentration of specific pore sizes (Figure 4B). The data was consistent with the traditionally prepared MIP$_{M2}$ possessing larger pores, and also with a significant difference between MW-MIP$_{M2}$ and MW-NIP$_{M2}$, and clear evidence of a template effect with significantly higher gas volume at higher pressure relative to

MW-NIP$_{M2}$. As the sole difference in synthesis approach was the use of microwaves, the method of MIP production clearly affects the nature of the polymeric material produced. In this instance, the MW-MIP$_{M2}$ displayed good imprinting, high rebinding

5 capacity and a narrow size distribution of pore sizes. This is consistent with our prior 'snap freezing' hypothesis.[46]
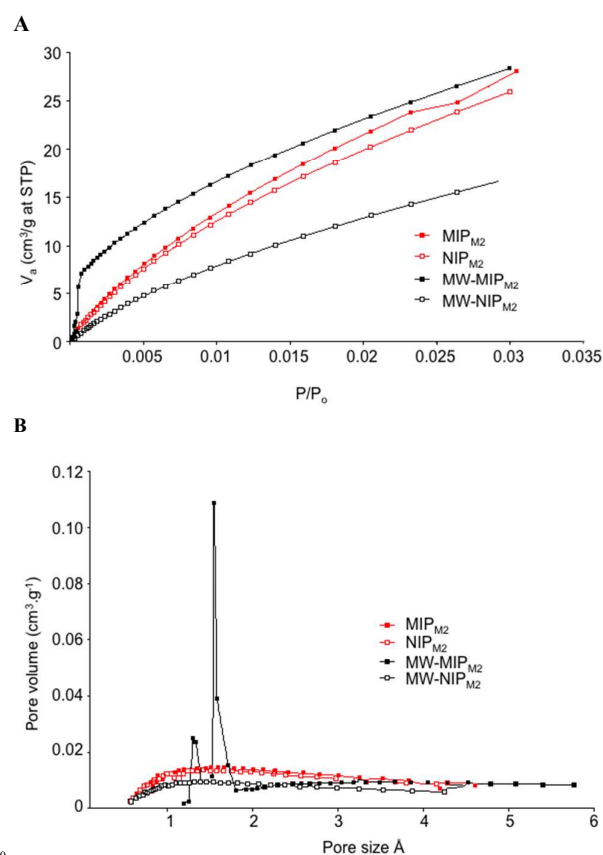
A

B

10

Figure 4. (**A**) Gas adsorption isotherms of MIP$_{M2}$ and NIP$_{M2}$ and MW-MIP$_{M2}$ and MW-NIP$_{M2}$. (**B**) Pore size distribution for MIP$_{M2}$ and NIP 2 and MW-MIP$_{M2}$ and MW-NIP$_{M2}$.

Albright suggested that MIP macroporosity arose due to the

15 formation of clusters of microgel that are fused together at their interface.[52,53] The meso and macroporosities are imparted by the voids within the clusters and the spaces between the microgels. A phase separation occurring rapidly during polymerisation, as in the case of microwave-induced polymerisation, will result in

20 more fused microgels, and consequently in lower surface areas than for a phase separation occurring later as in the case of thermal polymerisation. The observed specific surface areas of the MIP$_{M2}$ and NIP$_{M2}$ and MW-MIP$_{M2}$ and MW-NIP$_{M2}$ are consistent with Albright's model.[53] The thermal polymers

25 exhibited higher specific surface areas than the microwave-prepared polymers. The surface area effects partially rationalise the changes observed in IF, with the lower surface area anticipated to afford fewer sites for **1** to bind non-specifically to both the MW-NIP$_{M2}$ and MW-MIP$_{M2}$. The low pore sizes in

30 MW-MIP$_{M2}$ limits the degree of intra-polymer binding. However, measurement of their Zeta potentials revealed the surface charge of MW-NIP$_{M2}$ to be 40% lower than the surface charge of NIP$_{M2}$ which meant that adsorption of polar theophylline at the surface of MW-NIP$_{M2}$ would meet less

35 repulsion (i.e. be more favourable) compared to binding at the surface of NIP$_{M2}$ (Table 3).[54] Combined, these facets rationalise the lower IF observed with MW-MIP$_{M2}$, with the higher number

of specific surface imprinted sites allowing for higher levels of **1**-rebinding.

40 **Table 3.** BET surface area (m^2/g) of MIP$_{M2}$ and NIP$_{M2}$ and MW-MIP$_{M2}$ and MW-NIP$_{M2}$; and Zeta potential (mV) values of thermal and microwave polymers measured at pH 7.

Sample	Specific Surface Area (m^2/g)	Zeta Potential (mV)	IF/BET [a]
MIP$_{M2}$	240	-31.4 ± 4.8	0.0154
NIP$_{M2}$	228	-22.7 ± 2.9	
MW-MIP$_{M2}$	185	-13.1 ± 8.2	0.0124
MW-NIP$_{M2}$	162	-8.91 ± 3.43	

[a] calculated at 30 mg polymer, as this represents binding saturation point.

Normalising the IF values relative to surface area shows that

45 there is little difference in the selectively of MIP$_{M2}$ vs. MW-MIP$_{M2}$ with values of 0.0154 and 0.0124, respectively. However, as previously noted, there was a considerable difference in the rebinding capacity of these systems, with the microwave MIP exhibiting a 2-5 times greater capability to extract template-**1**.

50 This highlighted the effect of polymerisation mode, in this case, the use of microwave irradiation, on the selectivity of MW-MIP$_{M2}$'s, and was consistent with our previous finding with the preparation of theophylline and caffeine imprinted polymers prepared using microwave irradiation.[46]

55 The polymers produced in both modes of polymerisation are porous with the MIP$_{M2}$ and NIP$_{M2}$ as demonstrated by BET surface area and by examination of the SEM images of these polymers (Figure 5). There are observable differences in surface morphology between the thermal and microwave polymers, with

60 both MW-MIP$_{M2}$ and MW-NIP$_{M2}$ show rougher surfaces. This was not surprising considering that thermal polymerisation produced polymer monoliths that are more compact and harder than the microwave produced polymers.
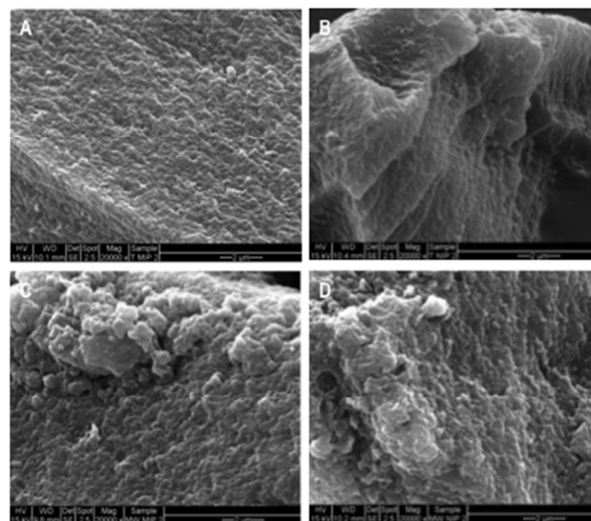

65 **Figure 5**. Scanning Electron micrographs of (**A**) MIP$_{M2}$, (**B**) NIP$_{M2}$, (**C**) MW-MIP$_{M2}$ and (**D**) MW-NIP$_{M2}$ at 20000x magnification showing the pore structure of the polymers.

Saturation Binding

The binding characteristics of both MIP$_{M2}$ and MW-MIP$_{M2}$

70 were compared through interrogation of the binding and Freundlich isotherms (Figure 6; and ESI†).[55,56] The Freundlich plot of microwave and thermal polymers, and each of their corresponding affinity distributions in semi log and log format facilitated calculation of N_T and K_d (K_a^{-1}), with the summary of

75 these binding parameters are presented in Table 4.

The Freundlich isotherm defines the amount bound (B) as a power function to the free concentration (F). The binding

4

parameter (*a*) is a measure of the number of binding sites (N_T) in the system and also equals the value of the affinity constant (K_a). On the other hand, *m* measures the heterogeneity of the system, with value ranges from 0 to 1, and it also measures the ratio of high affinity sites in the polymer. A heterogeneous system obtains a value of *m* close to 0 while an *m* value approaching 1 indicates increasing homogeneity
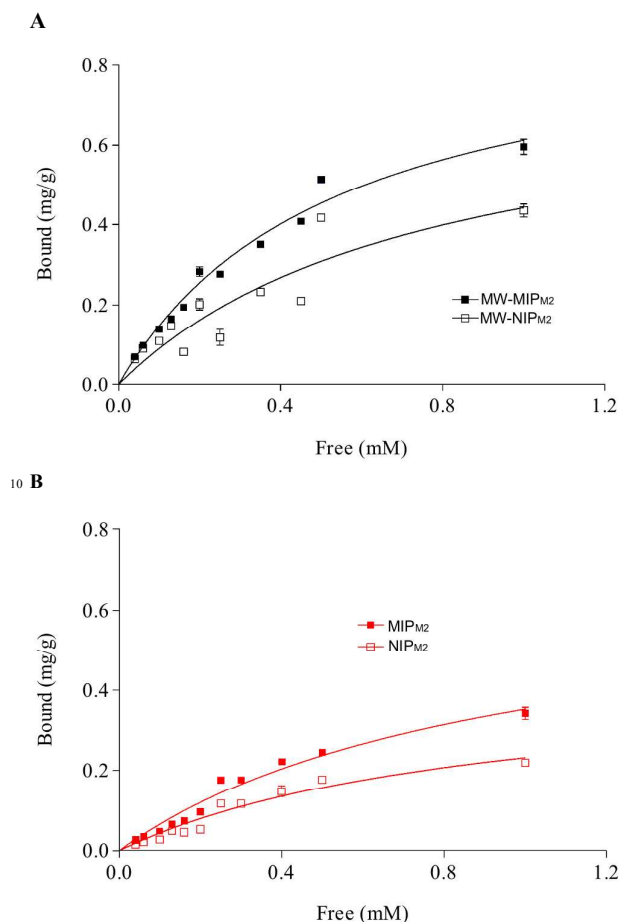
A

B

Figure 6. Binding isotherms generated for microwave (**A**) and thermal (**B**) MIP 2 and NIP 2. Thirty (30) mg of each polymer were incubated with increasing concentrations of theophylline ranging from 0.04 mM to 1.0 mM in acetonitrile for 2.0 h.

Table 4. K_d, N_T and m values obtained from Freundlich plots of the binding isotherms of thermal and microwave MIP$_{M2}$ and NIP$_{M2}$.

Polymer	Binding Parameters		
	K_d	N_T(mg/g)	m
MW-MIP$_{M2}$	1.38	0.72	0.71
MW-NIP$_{M2}$	2.43	0.41	0.59
MIP$_{M2}$	2.31	0.43	0.88
NIP$_{M2}$	3.38	0.30	0.93

The difference in the nature of the binding sites in each polymer was assessed by the heterogeneity index, m, obtained as the slope in the linear plot of the Freundlich isotherms. MW-MIP$_{M2}$ displayed an m value of 0.71 compared to 0.59 for MW-NIP$_{M2}$. This suggests that MW-MIP$_{M2}$ has a slightly more homogenous mix of affinity sites. The K_d value of MW-NIP$_{M2}$, on the other hand, is 1.8 times higher than MW-MIP$_{M2}$ (2.43 vs 1.38) which indicates that the binding sites in MW-MIP$_{M2}$ have a higher affinity for **1** than the binding sites in MW-NIP$_{M2}$, consistent with the expected imprinting effect. In addition, MW-MIP$_{M2}$ also exhibits a higher number of binding sites (N_T)

compared to MW-NIP$_{M2}$ (0.72 and 0.41 mg/g, respectively).

Analysis of the Freundlich isotherm also reveals MIP$_{M2}$ and NIP$_{M2}$ to have similar m values of 0.88 and 0.93, respectively, consistent with the MIP$_{M2}$ being more homogenous. The higher m value also indicates a more discrete distribution of affinity sites within the polymers than for the microwave polymers. The K_d value for MIP$_{M2}$ was 1.5 times that of NIP$_{M2}$ confirming the presence of template introduced high affinity sites. The MIP:NIP K_d ratio in both systems are comparable and suggest, that whilst the mode of polymerisation seems to influence the surface porosity and binding sites, as seen from the results of the BET measurements and the sorption studies, it does not have an apparent impact, as predicted by the MM-NMR studies, on the nature of the template-specific cavities formed during imprinting.

As with the MW polymers, MIP$_{M2}$ has a higher number of binding sites (N_T) than NIP$_{M2}$ however, MW-MIP$_{M2}$ displayed a higher N_T than MIP$_{M2}$. This is in agreement with the observed sorption behaviour of the MIPs towards **1** where MW-MIP$_{M2}$ bound more theophylline than MIP$_{M2}$. Similarly, MW-NIP$_{M2}$ displayed higher N_T than MIP$_{M2}$. In addition to the surface being more favourable for theophylline binding because of a low surface charge, i.e. zeta potential, it can also be speculated that the "snap freezing" effect of microwave polymerisation probably created a "functional group" specific cavity for theophylline. As mentioned earlier, microwave induced polymerisation has caused an alignment of polar groups in the solution, in this case the –NH from theophylline and the –OH from **M2**. Upon rapid microwave heating, which caused a faster polymerisation rate, this aligned –NH and OH functional groups could be "snap frozen" in the sub-surface of the polymer, creating a functional group specific cavity that can fit the –NH group of theophylline leaving the rest of the molecule exposed at the surface. This also explains the presence of a high distribution of micropore sizes in MW-MIP$_{M2}$ ($\leq$ 7Å), smaller than the diameter of theophylline.

Cross Reactivity and Selectivity Study

MIP$_{M2}$ and MW-MIP$_{M2}$ specificity for **1** was evaluated using **2** as a closely related analogue.[57] Both competitive binding (using **2** to compete with **1**) and selectivity studies (using two rebinding solution – one comprising solely **1** and the other solely **2**) were conducted and the outcomes are presented in Figure 7.

In rebinding experiments with 0.20 mM solution of **1** and **2**, separately, in CH$_3$CN, both MIP$_{M2}$ and MW-MIP$_{M2}$ rebound both **1** and **2**. MIP$_{M2}$ showed an approximately 2-fold preference for **1** over **2** and MW-MIP$_{M2}$ a 5-fold preference for rebinding **1** (Figure 7A). The quantity of **2** rebound by both MIP$_{M2}$ and MW-MIP$_{M2}$ was essentially identical suggestive of non-specific interaction with the polymer.
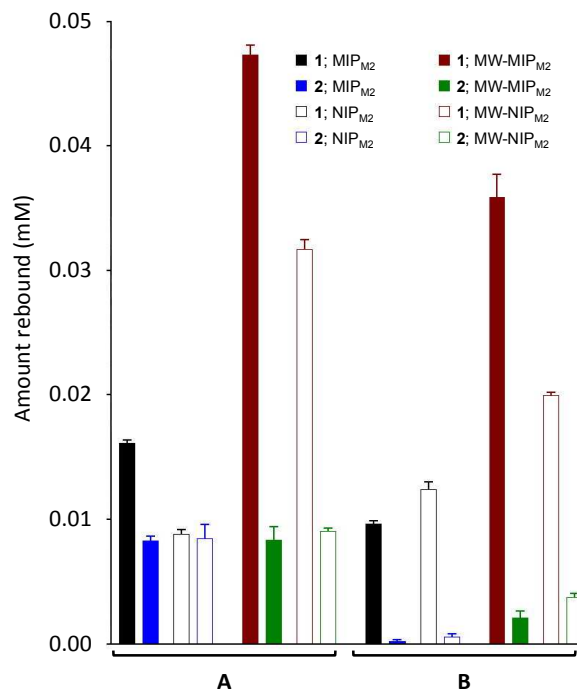
Figure 7. (A) Selective rebinding of **1** (■) and **2** (■) by MIP$_{M2}$ and rebinding of **1** (□) and **2** (□) by NIP$_{M2}$; and of **1** (■) and **2** (■) by MW-MIP$_{M2}$ and rebinding of **1** (□) and **2** (□) by NIP$_{M2}$. Rebinding conducted using 0.20 mM **1** in 1 mL CH$_3$CN and 0.20 mM **2** in 1 mL CH$_3$CN; (B) Cross-reactivity of **1** (■) and **2** (■) by MIP$_{M2}$ and rebinding of **1** (□) and **2** (□) by NIP$_{M2}$; and of **1** (■) and **2** (■) by MW-MIP$_{M2}$ and rebinding of **1** (□) and **2** (□) by NIP$_{M2}$. Rebinding conducted using 0.2 mM **1** and 0.20 mM **2** in 1 mL CH$_3$CN. MIPs were in contact with rebinding solutions for 2 h.

In the competitive rebinding experiments 0.20 mM **1** and 0.20 mM **2** in 1 mL of CH$_3$CN were treated with 30 mg of each MIP as before. In this instance the quantity of **1** and **2** rebound decreased relative to the first series of experiments, and this is most likely due to competition between **1** and **2** for the specific binding sites and potential self association at the higher compound concentration (0.40 vs. 0.20 mM total concentration). More significantly, both MIP$_{M2}$ and MW-MIP$_{M2}$ showed increased levels of discrimination between **1** and **2** with a clear preference for rebinding of **1** (Figure 7B).

Callahan *et al.*,[58] reported the formation of dimers by caffeine, detected as a strong signal from mass spectroscopy, while surprisingly, theophylline did not. However, it may be reasonable to assume that theophylline and caffeine may also interact in a similar fashion (to caffeine:caffeine) due to their structural similarity. Theophylline and caffeine may form a dimer in solution, thereby competing with MIP and thus resulting in reduced theophylline recognition without any otherwise obvious competition from caffeine.

Conclusion

The T-M interaction studies demonstrated that biphenyl monomers **M1-M6** were capable of interacting favourably with **1** via hydrogen bonding. Both molecular modelling and ^{1}H NMR spectroscopy approaches suggest that favourable T-FM interaction with minimal inter-monomer association can be achieved at T:FM ratios ≤ 1:4. Among the monomers studied, **M2** and **M6** gave the highest complex induced shifts, obtained from Job plots at a **1**-mol fraction < 0.5, and suggest that the interaction of **M2** and **M6** with **1** was stronger than with the other monomers.

Functional monomers **M1-M6** were used to synthesise MIPs for **1**. Of these, only MIP$_{M2}$ showed high affinity and selectivity for **1**. The same polymer synthesised using **M2** was prepared employing microwave polymerisation (MW-MIP$_{M2}$) to investigate the effect of the mode of polymerisation in the imprinted polymer. MW-MIP$_{M2}$ exhibited high affinity towards, and greater selectivity for **1** than the competing analyte (**2**) compared to MIP$_{M2}$.

The nature of binding sites obtained in the polymers is influenced by the mode of polymerisation. Thermal polymers obtained more homogenous binding sites because of the equilibrium driven thermal polymerisation, while microwave polymers resulted in a greater distribution of heterogeneous binding sites, which was attributed to the "snap freeze" polymerisation. However, the effect of microwave polymerisation leads to formation of micropores in the MW-MIP$_{M2}$ which is not evident in MW-NIP$_{M2}$ and the thermal polymers.

Experimental

General Experimental

All monomers used were synthesised as previously described in reference 36. Theophylline (**1**; anhydrous, ≥99%) and caffeine (**2**) were obtained from Sigma-Aldrich and were used as received. Ethylene glycol dimethacrylate (EGDMA), from Sigma Aldrich, was purified using aluminium oxide (activated, basic) prior to use. Azobisbutyronitrile (AIBN, Dupont) was recrystallised from acetone prior to use. HPLC grade (Fluka) dimethylformamide (DMF), acetonitrile (ACN) and methanol (MeOH) were used as received. Glacial acetic acid, triethylamine (TEA) and deuterated dimethylsulfoxide (DMSO) were obtained from Sigma-Aldrich and used as received.

Molecular Modelling

Template-monomer molecular interactions were modelled using Spartan '04 software using the AM1 force field.[59,60] This molecular orbital computational method predicts the stable configuration of the template (T), monomer (M), M-M clusters and T-M clusters and calculates their standard heats of formation (ΔH_f). The molecules were randomly positioned and the T-M clusters were modelled with respect to increasing the template-monomer ratio from 1 to 4. To account for the M-M interaction, the M-M clusters of up to five molecules were also surveyed. The energy of interaction of the T-M clusters, $\Delta E°_{(cluster)}$, at different molecular ratios were then calculated using the equation:

$$\Delta E_{interaction} = \Delta H_{f\ FM\text{-}T\ complex} - [\Delta H_{f\ monomer\ cluster} - \Delta H_{f\ template}].[61]$$

^{1}H NMR titration

Typically, from a stock solution of 500.0 mM in DMSO, incremental amounts of 50.0 µL of the biphenyl monomer was added to a 0.50 mL of 50.00 mM solution of **1** in deuterated DMSO. The proton signal from the NH and vinylic protons of theophylline were monitored as incremental amounts of monomers were added. The titration curve was then constructed from the plot of change in chemical shift, δ (ppm), of the NH and vinylic protons of theophylline against increasing amount of monomers added. All ^{1}H NMR measurements were made using NMR Brüker Avance 300 MHz.

Job Plots

Appropriate volumes of **1** (51.5 mM) and monomer (51.5 mM) stock solutions prepared in deuterated DMSO were combined in an NMR tube to make up 0.50 mL solution with the resulting **1**:**M1** (to **M6**) ratios of 10:0, 9:1, 8:2, 7:3, 6:4, 5:5, 4:6, 3:7, 2:8, 1:9 and 0:10. The proton signals from the NH and vinylic protons of **1** were followed and recorded. A Job plot was then constructed

from the plot of **1**-monomer complex-induced shift (ppm) of the NH and vinylic protons of **1** against the mole fraction of theophylline.

Polymer Synthesis

In a typical synthesis, molecularly imprinted polymers were prepared as follows. Pre-determined quantities of the template **1** (0.50 mmol, 90.08 mg), biphenyl monomer (**M1**) (1.00 mmol, 271.8 mg), EGDMA (10.00 mmol, 1.888 mL) and AIBN (1 mmol %, 35.3 mg) were dissolved in DMF (4.00 mL) in a 10-mL vial, purged with nitrogen gas for 5 min, sealed and polymerised at 60 ± 1.0 °C in a Thermoline oven for overnight. The polymers were then ground and sieved to a particle size <38 µm. The template was extracted via Soxhlet extraction in methanol:acetic acid (90:10 v/v) for 24 h and further washed in methanol for another 24 h.[10, 12] In some cases, a blank is run to check leaching of the template form the polymer.[62] The polymers were then dried at 40°C in a vacuum oven. A similar procedure was applied to non-imprinted polymers with the exception that no template was added.

Table 5. Formulation in the preparation of MIPs and NIPs.

Polymer[a]	monomer (mmol)	theophylline (mmol)	EGDMA (mmol)	DMF (mL)
MIP$_{M1}$	1.500	0.500	10.000	2.000
MIP$_{M2}$	1.000	0.250	5.000	2.000
MIP$_{M3}$	1.500	0.500	10.000	2.000
MIP$_{M4}$	1.000	0.500	10.000	2.000
MIP$_{M5}$	1.000	0.250	5.000	2.000
MIP$_{M6}$	1.000	0.500	10.000	2.000

[a]Polymerisation was conducted at 60 °C for 18 h. The same formulation was used for the preparation of NIP except in the addition of **1**.

For the microwave synthesis, a similar procedure was used as for the thermal synthesis, except that polymers were polymerised in a 10 mL pressure vessel via microwave heating using CEM Discoverer Benchmate at 60 ºC using 100W for 15 min.

Sorption Study

A Sorption study was performed using batch binding experiments where various amounts of polymers ranging from 10.0 to 50.0 mg were placed into a 5 mL vial to which was added 1.00 mL of 0.0800 mM theophylline in acetonitrile. The mixture was shaken for 18 h, filtered and the filtrate analysed directly by HPLC. The amount of free theophylline was subtracted from the initial binding solution concentration to obtain the amount of theophylline bound in the polymer. All binding experiments for this study were done in triplicate to ensure reproducibility. A sorption isotherm was generated from the plot of theophylline bound (mM) versus amount of polymer (mg).

Time-Binding Study

Thirty milligrams, the optimal weight obtained from the adsorption study, was used for determining the optimum time of template binding. To a set of triplicate of 30.0 mg of polymer, 1.00 mL of 0.0800 mM theophylline was added and the mixture shaken for a designated time of contact. The binding times investigated were 0.5, 2.0, 4.0, 7.0 and 18 hours. After binding, the mixtures were filtered and the filtrates analysed by HPLC. The amount of bound theophylline was then obtained by subtracting the amount of theophylline left in solution from the initial concentration. A plot of the amount of theophylline bound versus time of contact was generated to determine the optimum time of contact for binding theophylline.

Saturation Binding

The optimum weight and time of contact obtained from sorption and time-binding studies were used for the saturation binding experiments. A series of 30.0 mg of polymers were incubated with different concentrations of **1** for 2 h, after which, the mixtures were filtered and the filtrates analysed directly by HPLC. The amount of bound theophylline was then obtained by subtracting the amount of **1** left in solution from the initial concentration. A plot of bound template against free **1** concentration was then generated to visualise the saturation binding isotherm of the polymers.

Binding measurements

Rebinding of **1** was measured using a Shimadzu Prominence HPLC equipped with SPD-20A/M20A lamp and LC-20AD pump. Analyses were performed on an Econosphere C_{18} 5µ column (150 x 4.6 mm) using isocratic elution of MeOH:water (80:20, v/v, with 0.10 % TEA) at 1.00mL/min at 40ºC. The injection volume used was 10 µL and the chromatograms were recorded at 254 nm and the peak at 1.25 min attributed to theophylline was measured.

A five-point calibration curve from five standard concentrations of theophylline with linear regression values (R^2) of 0.9996 was used to determine the concentrations of theophylline after binding measurements.

Scanning Electron Microscopy

Morphology of the polymers was examined using a Phillips XL30 scanning electron microscope. Each polymer was deposited on a sticky carbon tab and coated with gold using a SPI gold spotter coating unit. SEM micrographs of the polymers were obtained at 20000x magnification at 15.0 kV.

Swelling Measurements

Thirty milligrams of each polymer were packed into an NMR tube and the height of the dry polymer measured. A solution of theophylline (1.00 mL of 0.0800 mM) in acetonitrile was added and allowed to soak for 24 h. Polymers were allowed to settle and the bed height of the swollen polymers was measured. The swelling factor was calculated from the ratio of the bed height of the swollen polymer to the dry polymer.

Zeta Potential

Zeta potential measurements were performed using a Malvern Nanosizer S fitted with a maintenance-free folded capillary cell (DTS 1060). Very dilute suspensions of polymers were prepared using ~ 0.75 mL deoxygenated distilled deionized water (non-equilibrated in air, 18.2 MΩ cm⁻¹). Measurements were performed at 25.0 °C, pH 7.0 in 5 replicates.

Specific Surface Area and Porosity (Brunauer-Emmett-Teller)

Gas adsorption analysis was carried out using a Micrometrics ASAP 2020 Accelerated Surface Area and Porosity instrument (Norcross, GA, USA). The analysis was carried out using 100 mg of sample and degassed at 110ºC under vacuum for 12 h to remove any adsorbed solvent and water. The adsorption isotherm of this degassed sample was then measured using carbon dioxide as the adsorbate at a temperature of 500°C covering the partial pressure (P/P_0) range 1×10^{-6} to 0.03. The specific surface area of each sample was determined from the adsorption data using the linearised BET equation,[50] while the pore size distribution was calculated using the BJH (Barrett, Joyner & Halenda) model.

References

1. K. Mosbach and O. Ramström, *Nature Biotech.*, 1996, **14**, 163.
2. R. Arshady and K. Mosbach, *Macromol. Chem. Phys.*, 1981, **182**, 687.
3. G. Wulff and A. Sarhan, *Angew. Chem., Int. Ed. Engl.*, 1972, **11**, 341-348.
4. A. McCluskey, C. I. Holdsworth and M. C. Bowyer, Org. Biomol. Chem., 2007, 5, 3233.
5. A. Murray and B. Ormeci, *Environ. Sci. Pollut. Res. Int.,* 2012, **19**, 3820.
6. D. Yu, Y. Zeng, Y. Qi, T. Zhou and G. Shi, *Biosens. Bioelectron.*, 2012, **38**, 270.
7. A. Abouzarzadeh, M. Forouzani, M. Jahanshahi and N. Bahramifar, *J. Mol. Recognit.,* 2012, **25**, 404.
8. K. Farrington, E. Magner and F. Regan, *Anal. Chim. Acta,* 2006, **566**, 60.
9. H. Kempe and M. Kempe, *Anal. Bioanal. Chem.,* 2010, **396**, 1599.
10. L. Ye, K. Yoshimatsu, D. Kolodziej, J. D. C. Francisco and E. S. Dey, *J. Appl. Polym. Sci.,* 2006, **102**, 2863.
11. Y. Diñeiro, I. Menéndez, C. Blanco-López, J. Lobo-Castañón, A. J. Miranda-Ordieres and P. Tuñón-Blanco, *Biosens. Bioelectron.,* 2006, **22**, 364.
12. C. I. Holdsworth, M. C. Bowyer, C. Lennard and A. McCluskey, *Aus. J. Chem.,* 2005, **58**, 315.
13. K. Karim, F. Brenton, R. Rouillon, E. V. Piletska, A. Guerreiro, I. Chianella and S. A. Piletsky, *Adv. Drug Delivery Rev.,* 2005, **57**, 1795.
14. A. G. Mayes and M. J. Whitcombe, *Adv. Drug Delivery Rev.,* 2005, **57**, 1742.
15. K. Haupt, A. V. Linares, M. Bompart and B. T. Bui, *Topp. Curr. Chem.*, 2012, **325**, 1.
16. F. Puoci, G. Cirillo, M. Curcio, O. I. Parisi, F. Iemma and N. Picci, *Exp. Opin. Drug Deliv.,* 2011, **8**, 1379.
17. F. Puoci, F. Iemma and N. Picci, *Curr. Drug Deliv.,* 2008, **5**, 85-96.
18. Y. Fuchs, O. Soppera and K. Haupt, *Anal. Chim. Acta.*, 2012, **717**, 7.
19. O. Bruggemann, K. Haupt, L. Ye, E. Yilmaz and K. Mosbach, *J. Chromatogr., A*, 2000, **889**, 15.
20. S. G. Bertolotti, C. M. Previtali, A. M. Rufs and M. V. Encinas, *Macromolecules*, 1999, **32**, 2920.
21. S. R. Carter and S. Rimmer, *IEE Proc. Nanobiotechnol.*, 2005, **152**, 169.
22. T. A. Sergeyeva, S. A. Piletsky, A. A. Brovko, E. A. Slinchenko, L. M. Sergeyeva and A. V. Elskaya, *Anal. Chim. Acta*, 1999, **392**, 105.
23. T. A. Sergeyeva, S. A. Piletsky, A. A. Brovko, E. A. Slinchenko, L. M. Sergeyeva and A. V. El'skaya, *Analyst*, 1999, **124**, 331.
24. T. A. Sergeyeva, O. O. Brovko, E. V. Piletska, S. A. Piletsky, L. A. Goncharova, L. V. Karabanova, L. M. Sergeyeva and A. V. El'skaya, *Anal. Chim. Acta.*, 2007, **582**, 311.
25. P. A. G. Cormack and A. Z. Elorza, *J. Chrom. B,* 2004, **804**, 173.
26. Y. Zhang, D. Song, L. M. Lanni and K. D. Shimizu, *Macromol.,* 2010, **43**, 6284.
27. L. Schwarz, C. I. Holdsworth, A. McCluskey, and M. C. Bowyer, *Aus. J. Chem.*, 2004, **57**, 759.
28. L. J. Schwarz, B. Danylec, S. J. Harris, R. I. Boysen, M. T. W. Hearn, *J. Chrom. A* 2011, **1218**, 2189.
29. S. A. Piletsky, K. Karim, E. V. Piletska, C. J. Day, K. W. Freebairn, C. Legge and A. P. F. Turner, *Analyst* 2001, **126**, 1826.
30. L. Feng, B. Pamidighantam and P. Lauterbur, *Anal. Bioanal. Chem.,* 2010, **396**, 1607.
31. Y. Hu, Y. Li, R. Liu, W. Tan and G. Li, *Talanta* 2011, **84**, 462.
32. N. W. Turner, M. C. Bowyer, A. McCluskey and C. I. Holdsworth, *Aus. J. Chem.*, 2012, **65**, 1405.
33. L. I. Andersson, R. Muller, G. Vlatakis, G. and K. Mosbach,, Porc. Natl. Acad. Sci., 1995, **92**, 4788.
34. G. Vlatakis, L. I. Andersson, R., Muller, K. Mosbach, Nature, 1993, **361**, 645.
35. K. U. Walter, K. Vamvaca and D. Hilvert, *J. Biol. Chem.*, 2005, **280**, 37742.
36. H. A. Zayas, M. C. Bowyer, C. P. Gordon, C. I. Holdsworth and A. McCluskey, *Tet. Lett.*, 2009, **50**, 5894.
37. A. J. J. Wood, M. Weinberger and L. Hendeles, *New Eng. J. Med.,* 1996, **334**, 1380.
38. W. M. Mullett and E. P. C. Lai, *Anal. Chem.,* 1998, **70**, 3636.
39. W. M. Mullett, and E. P. C. Lai, *J. Pharm. Biomed. Anal.,* 1999, **21**, 835.
40. G. Vlatakis, L. I. Andersson, R. Muller and K. Mosbach, *Nature* 1993, **361**, 645.
41. A. R. Khorrami and A. Rashidpur, *Biosen. Bioelect.* 2009, **25**, 647.
42. C. M. Philip and B. Mathew, *J. Macromol. Sci., Part A: Pure App. Chem.,* 2008, **45**, 335.
43. J. Wang, P. A. G. Cormack, D. C. Sherrington and E. Khoshdel, *Angew. Chem. Int. Ed.,* 2003, **42**, 5336.
44. D. Wang, S. Hong and K. Row, *Kor. J. Chem. Eng.,* 2004, **21**, 853.
45. M. C. Norell, H. S. Andersson and I. A. Nicholls, *J. Mol. Recog.,* 1998, **11**, 98.
46. N. W. Turner, C. I. Holdsworth, S. W. Donne, A. McCluskey and M. C. Bowyer, *New J. Chem.* 2010, **34**, 686.
47. Y. Lu, C. Li, X. Wang, P. Sun and X. Xing, *J. Chrom. B* 2004, **804**, 53.
48. Spivak, D. A. *Adv. Drug Deliv. Rev.*, 2005, **57**, 1779.
49. D. Spivak, *Molecular Imprinting Technology*. In Smart Materials, CRC Press: 2008.
50. S. Brunauer, P. H. Emmett and E. Teller, *J. Am. Chem. Soc.* 1938, **60**, 309.
51. S. Lowell, Adsorption isotherm. *Characterization of porous solids and powders: surfaces, pore size, and denisty.* Kluwer Academic Publisher 2004.
52. H. Deleuze, X. Schultze and D. C. Sherrington, *Polym. Bull.,* 2000, **44**, 179.
53. R. L. Albright, *React. Poly. Ion Exch., Sorbents* 1986, **4**, 155.
54. A. I. Liapis and G. A. Grimes, *J. Sep. Sci.,* 2007, **30**, 648.
55. R. J. Umpleby, S. C. Baxter, M. Bode, J. K. Berch, R. N. Shah and K. D. Shimizu, *Anal. Chim. Acta* 2001, **435**, 35.
56. C. Brisbane, A. McCluskey, M. C. Bowyer and C. I. Holdsworth, *Org. Biomol. Chem.*, 2013, **11**, 2872.
57. K. Mosbach, *Trends Biochem. Sci.* 1994, **19**, 9.
58. M. P. Callahan, Z. Gengeliczki, N. Svadlenak, H. Valdes, P. Hobza, and M. S. de Vries, *PhysChem. ChemPhys.*, 2008, **10**, 2819.
59. M. J. S. Dewar, E. G. Zoebisch, E. F. Healy, J. J. P. Stewart, *J. Am. Chem. Soc.*, 1985, **107**, 3902.
60. Spartan '04, Wavefunction, Inc., Irvine California USA.
61. L. Schwarz, M. C. Bowyer, C. I. Holdsworth and A. McCluskey, *Aus. J. Chem.*, 2006, **59**, 129.
62. C. M. Phillip and B. Mathew, *J. Macromol. Sci., Part A: Pure Appl. Chem.*, 2008, **45**, 335.

[a] *Discipline of Chemistry, University of Newcastle, Callaghan, NSW 2308, Australia. Fax:+61 2 4921 5472; Tel: +61 2 4921 5472; E-mail: Adam.McCluskey@Newcastle.edu.au*
[b] *Discipline of Applied Sciences, School of Environmental & Life Sciences, University of Newcastle, Ourimbah, NSW 2258, Australia*

‡ Footnotes should appear here. These might include comments relevant to but not central to the matter under discussion, limited experimental and spectral data, and crystallographic data.